J. Astrophys. Astr. (1995) **16**, 375–391

A Numerical Survey of Neutron Star Crustal Density Profiles

B. Datta[1,3], A. V. Thampan[1] & D. Bhattacharya[2]
[1] *Indian Institute of Astrophysics, Bangalore 560 034, India.*
[2] *Raman Research Institute, Bangalore 560 080 India.*
[3] *Visiting Professor: Raman Research Institute, Bangalore 560 080 India.*

Received 1995 June 17; accepted 1995 August 14

Abstract. An accurate numerical survey of the density profiles corresponding to the crusts of neutron stars for representative equation of state models is presented. This will find application in calculations of thermal and magnetic evolution of neutron stars.

Key words: Stars: neutron—crusts: neutron star.

1. Introduction

The crust of a neutron star refers to a region, near the surface, that is composed of mainly neutron-rich bare nuclei which interact electrostatically and are arranged in a lattice. The outer crust has small admixtures of free electrons and the inner crust has, in addition to electrons, 'drip' neutrons populating continuum states and permeating the nuclear lattice space. With increasing depth from the surface, and hence with increasing density, the neutron-to-proton ratio of the nuclei increases till a point is reached where the nuclei 'dissolve' and the composition is largely a homogeneous sea of neutrons. This point is characterized as the crust bottom. Although the crusts comprise a relatively small fraction of the total radius of the neutron star (usually about 10%), their importance derives from the fact that these possess interesting transport properties, and are believed to play a central role in a variety of directly and indirectly observable properties of neutron stars. The former include glitches, X-ray emission, and the latter concern the evolution of neutron star magnetic fields (and hence the evolution of pulsars) and possible changes in the neutron star structure and composition due to long-term accretion from a binary companion star. In order to understand all these and related phenomena quantitatively, it is imperative to have accurate knowledge of the radial distribution of the density in the crust.

Calculations suggest that neutron stars possess a more or less flat density profile from the centre to the crust bottom (Arnett & Bowers 1977; Datta 1988), and that the crust contains negligible mass in comparison to the mass in the rest of the star. The crust bottom (which is the boundary layer between the inner crust and the interior region) according to realistic calculations, is roughly equal to the equilibrium nuclear matter density, $\simeq 2.4 \times 10^{14}\,\mathrm{g\,cm^{-3}}$. This is about an order of magnitude less than the central densities obtained in neutron stars. Across the crust, however, the density drop is extremely sharp – about fourteen orders of magnitude. Clearly, an accurate knowledge of the crustal density profile needs an accurate numerical treatment while integrating the equilibrium structure equations in this region of extremely rapid density

variation. The equation of state (EOS) of neutron star matter is the key input parameter in all these calculations, the crustal properties depending sensitively on which particular EOS model is adopted to describe the neutron star interior. In general, the stiffer the EOS, the more the extent of the crust. In this paper, we present a numerical survey of crustal density profiles for several neutron star configurations, and for a representative choice of the EOS models.

2. Equations of state

The structure of neutron star depends sensitively on the EOS at high densities. Although the main composition of degenerate matter at densities $\gtrsim 2.4 \times 10^{14}\,\mathrm{g\,cm^{-3}}$, that characterize neutron star interiors, is expected to be dominated by neutrons, significant admixtures of other elementary particles (such as pions, muons and hyperons) are not ruled out. A persistent problem in determining the EOS (namely, pressure as a function of density) of such high density matter is what to choose for the interaction among the various particles, for which reliable experimental information is not available. All calculations involve either extrapolations from known nuclear matter properties or field theoretical approaches. Another unresolved problem is: what many-body technique is adequate for the purpose of evaluating the higher order correlation terms for the pressure. In this paper we do not address these problems, but choose for our purpose, eight EOS models based on representative neutron star matter interaction models. A brief description of these is given below.

A. Pandharipande (neutron matter): Pandharipande (1971a) studied behaviour of dense neutron matter using a many-body theory based upon the variational approach suggested by Jastrow (1955). The two-body wave function was taken as satisfying a simplified form of the Bethe-Goldstone equation, in which, terms representing the Pauli exclusion principle were omitted but simulated by imposing a 'healing' constraint on the wave function. Instead of a state-dependent correlation function, an average was used with spin dependence. To describe the nuclear interaction, the Reid nucleon-nucleon potential was used (Reid 1968). This potential model is now considered to be inadequate as it does not fully describe known nuclear matter properties.

B. Pandharipande (hyperonic matter): At high densities that prevail in neutron star interiors, it is possible that elementary particles heavier than neutrons, such as hyperons, may also be present. The suggestion that hyperons may be additional baryonic constituents of neutron star interiors was first made by Ambartsumyan & Saakyan (1960) based on energetic arguments. Although our knowledge of hyperonic interactions is meagre (primarily because of lack of experimental data), there have been several theoretical attempts aimed at deriving the EOS of baryonic liquid made up of neutrons, protons, hyperons ($\Lambda, \Sigma^{\pm 0}$). One of the early such attempts is due to Pandharipande (1971b), who assumed the hyperonic potentials to be similar to the nucleon-nucleon potentials, but altered suitably to represent the different isospin states. The many-body method adopted to derive the EOS was similar as in the case A. Several EOS models of hyperonic matter have since been proposed by different authors. However, this still remains an open problem because our knowledge of hyperon-nucleon and hyperon-hyperon interactions and their coupling constants have large uncertainties.

C. Bethe-Johnson: Bethe & Johnson (1974) devised phenomenological potentials for nucleon-nucleon interaction that have more realistic short-range behaviour than the Reid potentials. These authors then used the lowest order constrained variational method as given by Pandharipande (1971a) to calculate the EOS of neutron star matter. The work of Bethe & Johnson (1974) consists of two different parts: (1) determination of the EOS for a pure neutron gas and (2) derivation of a hyperonic equation of state. For purpose of illustration here, we have chosen their EOS model V (neutron matter).

D. Walecka: The exchange of vector and scalar mesons among nucleons is known to provide the short-range repulsion and intermediate-range attraction in the nucleon-nucleon potential. The effective interaction will be characterized by the meson parameters, such as their masses and coupling constants. If these parameters are specified, the meson wave functions can be easily solved as a function of density (assuming the wave functions to be space-time independent). From this, one can evaluate the stress tensor, which then provides the EOS. Walecka (1974) chose the meson parameters so as to reproduce the binding energy of nuclear matter (assumed to be -15.75 MeV/nucleon) at a saturation density of 0.193 nucleons fm^{-3}. More recent analysis of experimental data suggests the nuclear matter binding energy to be -16.3 MeV/nucleon and a saturation density of 0.153 nucleons fm^{-3} (Möller *et al.* 1988). The EOS model of Walecka corresponds to pure neutron matter. Both the scalar and vector mesons are assumed to have zero isospin by Walecka, so the model does not give the right asymmetry energy for nuclear matter.

E. Friedman-Pandharipande (neutrons): This model (Friedman & Pandharipande 1981), is also based on the lowest order constrained variational method. However, instead of the Reid potentials, the authors have made use of an improved phenomenological nucleon-nucleon potential containing a two-body part as well as three-body correlations. This interaction fits the nucleon-nucleon scattering cross-section data, deuteron properties, and also the nuclear matter properties rather well.

F. Wiringa, Fiks & Fabrocini (1988): These authors gave a model of EOS for dense nuclear and neutron matter which includes three-nucleon interactions. This is a non-relativistic approach based on the variational method. The three-body potential considered by the authors includes long-range repulsive parts that are adjusted to give light nuclei binding energies and nuclear matter saturation properties. This work represents an improvement over the calculation of Friedman & Pandharipande (1981) regarding the long-range attraction term in the Hamiltonian. The authors have given three models. We consider here their model for beta-stable case: UV14 + UVII (neutrons, protons, electrons and muons).

G. Prakash, Ainsworth & Lattimer (1988) proposed EOS models for neutron stars, based on an extrapolation of the energy per particle of symmetric nuclear matter. The approach is empirical, and involves several parameters. The total energies are obtained by inclusion of the nucleon kinetic energy and the effect of finite forces between nucleons. Four models have been suggested by the authors; we use model 1 for our purpose.

H. Sahu, Basu & Datta (1993) gave a field theoretical EOS for neutron-rich matter in beta equilibrium based on the chiral sigma model. The model includes an isoscalar vector

field generated dynamically and reproduces the empirical values of the nuclear matter saturation density and binding energy and also the isospin symmetry coefficient for asymmetric nuclear matter. The energy per nucleon of nuclear matter according to Sahu, Basu & Datta (1993) is in very good agreement, up to about four times the equilibrium nuclear matter density, with estimates inferred from heavy-ion collision experimental data.

Models A, B and G are relatively soft EOS, models E, C and F are roughly intermediate in their stiffness whereas models D and H are very stiff EOS. The composite EOS for the entire span of neutron star densities was constructed by joining the selected high density EOS to that of Negele & Vautherin (1973) for the density range $(10^{14} - 5 \times 10^{10})\,\mathrm{g\,cm^{-3}}$, Baym, Pethick & Sutherland (1971) for densities down to $\sim 10^{3}\,\mathrm{g\,cm^{-3}}$ and Feynman, Metropolis & Teller (1949) for densities less than $10^{3}\,\mathrm{g\,cm^{-3}}$.

3. Calculations

The Tolman-Oppenheimer-Volkoff (Oppenheimer & Volkoff 1939) equations that must be integrated numerically to obtain stable, non-rotating neutron star structure are:

$$\frac{dm}{dr} = 4\pi r^2 \rho \tag{1}$$

$$\frac{dP}{dr} = -\frac{G(m + 4\pi r^3 P/c^2)(\rho + P/c^2)}{r(r - 2Gm/c^2)}, \tag{2}$$

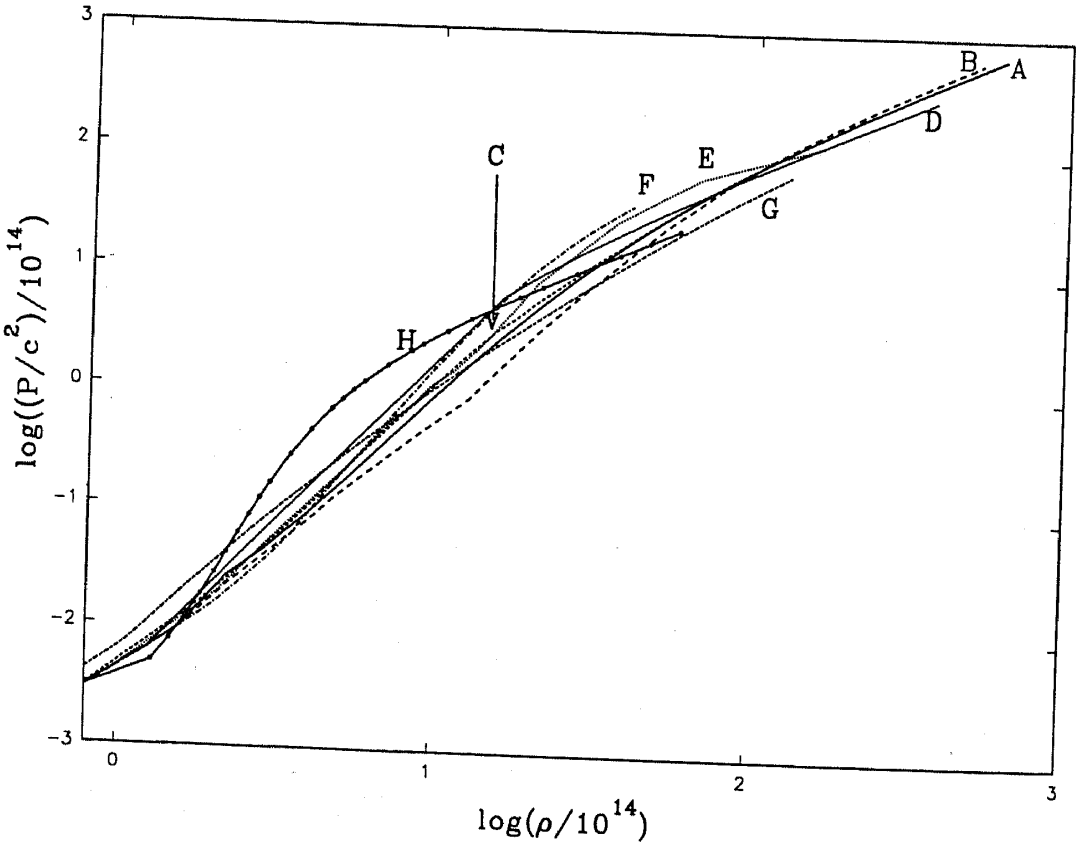

Figure 1. Pressure as a function of density for the EOS models (A–H).

Table 1. Neutron star structure parameters for the EOS Models (A–H).

EOS	$M/M_\odot$	R (km)	ρ_c (g cm^{-3})	Δ (km)	M_{cr}/M
Pandharipande (neutrons)	1.330	10.006	$1.669E+15$	0.963	$3.024E-02$
	1.400	09.867	$1.830E+15$	0.858	$2.537E-02$
	1.658	08.492	$4.100E+15$	0.404	$8.031E-03$
Pandharipande (hyperons)	1.330	07.921	$3.606E+15$	0.484	$9.189E-03$
	1.400	07.437	$4.795E+15$	0.361	$5.863E-03$
	1.414	07.082	$6.017E+15$	0.300	$4.426E-03$
Bethe-Johnson Model V (neutrons)	1.330	10.782	$1.283E+15$	1.149	$3.945E-02$
	1.400	10.691	$1.373E+15$	1.044	$3.411E-02$
	1.758	09.200	$3.466E+15$	0.454	$9.565E-03$
Walecka	1.330	12.252	$7.158E+14$	1.442	$5.482E-02$
	1.400	12.280	$7.415E+14$	1.387	$5.415E-02$
	2.285	11.216	$2.174E+15$	0.452	$1.040E-02$
Friedman-Pandharipande (neutrons)	1.330	10.824	1.332E+15	1.134	3.859E-02
	1.400	10.701	1.413E+15	1.023	3.297E-02
	1.986	09.028	3.450E+15	0.307	5.531E-03
Wiringa *et al.* (UV14 + UVII)	1.330	11.122	$1.000E+15$	1.120	$3.543E-02$
	1.400	11.115	$1.043E+15$	1.039	$3.167E-02$
	2.189	09.800	$2.830E+15$	0.294	$4.946E-03$
Prakash, Ainsworth & Lattimer Model 1	1.330	11.384	$1.507E+15$	1.702	$7.376E-02$
	1.400	10.987	$1.808E+15$	1.456	$5.781E-02$
	1.510	09.483	$3.590E+15$	0.901	$2.744E-02$
Sahu, Basu & Datta	1.330	14.685	$3.952E+14$	3.128	$2.518E-01$
	1.400	14.761	$4.063E+14$	2.970	$2.342E-01$
	2.593	14.096	$1.345E+15$	0.975	$4.588E-02$

NOTE: In Tables 1–9, the numbers following the letter E represent powers of ten.

where P and ρ stand for pressure and density and m is the gravitational mass contained within a sphere of radius r. The integration of equations (1) and (2) is done for a given EOS which specifies $P(\rho)$, and with initial condition $\rho = \rho_c$, a chosen value for the central density. The numerical integration started from the centre of the star is terminated at the radius of the star, defined as the point where the density $\lesssim 7.86\,\mathrm{g\,cm^{-3}}$, expected to correspond to the neutron star surface. The total gravitational mass is then given by $M = m(R)$.

We integrate equations (1) and (2) simultaneously using Runge-Kutta fourth order method, having an adaptive step size control. The step size is adjusted for the required accuracy from a calculation of the local truncation error (Antia 1991). We find that this provides an extremely accurate method to integrate equations (1) and (2) for neutron

Table 2. Crustal density profiles: Pandharipande (neutrons).

$M = 1.330\ M_\odot$, $R = 10.006$ (km)		$M = 1.400\ M_\odot$, $R = 9.867$ (km)		$M = 1.658\ M_\odot$, $R = 8.492$ (km)	
$(1 - r/R)$	ρ (g cm^{-3})	$(1 - r/R)$	ρ (g cm^{-3})	$(1 - r/R)$	ρ (g cm^{-3})
$0.00000E+00$	$7.866E+00$	$0.00000E+00$	$7.863E+00$	$0.00000E+00$	$7.866E+00$
$1.13773E-09$	$1.319E+01$	$1.28891E-09$	$1.360E+01$	$9.91795E-10$	$1.447E+01$
$2.39423E-08$	$4.972E+01$	$2.23090E-08$	$5.120E+01$	$1.27579E-08$	$5.428E+01$
$1.41172E-07$	$1.874E+02$	$1.31095E-07$	$1.927E+02$	$7.44405E-08$	$2.037E+02$
$6.75515E-07$	$7.066E+02$	$6.21865E-07$	$7.252E+02$	$3.46816E-07$	$7.642E+02$
$2.35836E-06$	$2.664E+03$	$2.17080E-06$	$2.730E+03$	$1.19743E-06$	$2.867E+03$
$6.95373E-06$	$1.004E+04$	$6.34094E-06$	$1.027E+04$	$3.47397E-06$	$1.076E+04$
$1.94642E-05$	$3.786E+04$	$1.77038E-05$	$3.866E+04$	$9.73952E-06$	$4.037E+04$
$5.14517E-05$	$1.427E+05$	$4.67151E-05$	$1.455E+05$	$2.53765E-05$	$1.515E+05$
$1.26075E-04$	$5.382E+05$	$1.14160E-04$	$5.477E+05$	$6.23815E-05$	$5.683E+05$
$2.88548E-04$	$2.029E+06$	$2.60880E-04$	$2.061E+06$	$1.40445E-04$	$2.132E+06$
$6.06912E-04$	$7.649E+06$	$5.47153E-04$	$7.758E+06$	$2.93273E-04$	$8.001E+06$
$1.14403E-03$	$2.884E+07$	$1.03012E-03$	$2.920E+07$	$5.56213E-04$	$3.002E+07$
$2.05310E-03$	$1.087E+08$	$1.84738E-03$	$1.099E+08$	$9.86545E-04$	$1.126E+08$
$3.46132E-03$	$4.099E+08$	$3.11233E-03$	$4.136E+08$	$1.65994E-03$	$4.226E+08$
$5.44170E-03$	$1.545E+09$	$4.89128E-03$	$1.557E+09$	$2.61038E-03$	$1.586E+09$
$8.57267E-03$	$5.826E+09$	$7.70080E-03$	$5.859E+09$	$4.10792E-03$	$5.950E+09$
$1.28894E-02$	$2.196E+10$	$1.15691E-02$	$2.205E+10$	$6.20721E-03$	$2.233E+10$
$1.89605E-02$	$8.280E+10$	$1.70260E-02$	$8.299E+10$	$9.14044E-03$	$8.377E+10$
$2.54733E-02$	$3.122E+11$	$2.28786E-02$	$3.124E+11$	$1.22832E-02$	$3.143E+11$
$3.04385E-02$	$1.177E+12$	$2.73482E-02$	$1.176E+12$	$1.47004E-02$	$1.179E+12$
$3.39494E-02$	$4.437E+12$	$3.05103E-02$	$4.425E+12$	$1.64164E-02$	$4.425E+12$
$4.02999E-02$	$1.673E+13$	$3.62239E-02$	$1.665E+13$	$1.94675E-02$	$1.660E+13$
$5.34854E-02$	$6.306E+13$	$4.81026E-02$	$6.268E+13$	$2.59768E-02$	$6.230E+13$
$9.62614E-02$	$2.400E+14$	$8.69610E-02$	$2.400E+14$	$4.75309E-02$	$2.400E+14$

Note: In the crustal density profiles presented here and in the subsequent tables, the third mass column corresponds to that of the maximum stable mass.

star configurations varying widely in their density profiles. The method, of course, gives bulk properties such as masses, radii and moments of inertia that agree with the values already reported in the literature.

Table 3. Crustal density profiles: Pandharipande (hyperons).

$M = 1.330\ M_\odot$ $R = 7.921$ (km)		$M = 1.400\ M_\odot$ $R = 7.437$ (km)		$M = 1.658\ M_\odot$ $R = 7.082$ (km)	
$(1 - r/R)$	ρ (g cm^{-3})	$(1 - r/R)$	ρ (g cm^{-3})	$(1 - r/R)$	ρ (g cm^{-3})
$0.00000E+00$	$7.869E+00$	$0.00000E+00$	$7.873E+00$	$0.00000E+00$	$7.872E+00$
$1.07340E-09$	$1.386E+01$	$5.54109E-10$	$1.310E+01$	$7.30479E-10$	$1.386E+01$
$1.67489E-08$	$5.212E+01$	$1.22270E-08$	$4.937E+01$	$1.14305E-08$	$5.206E+01$
$9.81838E-08$	$1.959E+02$	$7.20507E-08$	$1.861E+02$	$6.69361E-08$	$1.956E+02$
$4.63059E-07$	$7.366E+02$	$3.44856E-07$	$7.013E+02$	$3.15345E-07$	$7.349E+02$
$1.61124E-06$	$2.769E+03$	$1.21581E-06$	$2.643E+03$	$1.09890E-06$	$2.761E+03$
$4.69519E-06$	$1.041E+04$	$3.55792E-06$	$9.961E+03$	$3.19785E-06$	$1.037E+04$
$1.31881E-05$	$3.914E+04$	$1.00363E-05$	$3.754E+04$	$8.98933E-06$	$3.898E+04$
$3.44931E-05$	$1.471E+05$	$2.63282E-05$	$1.415E+05$	$2.34770E-05$	$1.464E+05$
$8.49483E-05$	$5.531E+05$	$6.51209E-05$	$5.333E+05$	$5.78740E-05$	$5.502E+05$
$1.92058E-04$	$2.079E+06$	$1.47600E-04$	$2.010E+06$	$1.30595E-04$	$2.067E+06$
$4.02430E-04$	$7.817E+06$	$3.11479E-04$	$7.575E+06$	$2.74208E-04$	$7.767E+06$
$7.63318E-04$	$2.939E+07$	$5.91571E-04$	$2.855E+07$	$5.20308E-04$	$2.918E+07$
$1.35630E-03$	$1.105E+08$	$1.05199E-03$	$1.076E+08$	$9.30193E-04$	$1.096E+08$
$2.28591E-03$	$4.153E+08$	$1.77814E-03$	$4.056E+08$	$1.55724E-03$	$4.120E+08$
$3.59396E-03$	$1.561E+09$	$2.80054E-03$	$1.529E+09$	$2.45039E-03$	$1.548E+09$
$5.66066E-03$	$5.870E+09$	$4.42319E-03$	$5.761E+09$	$3.86507E-03$	$5.815E+09$
$8.55549E-03$	$2.207E+10$	$6.70178E-03$	$2.171E+10$	$5.85049E-03$	$2.185E+10$
$1.25852E-02$	$8.296E+10$	$9.87052E-03$	$8.183E+10$	$8.61429E-03$	$8.209E+10$
$1.70822E-02$	$3.119E+11$	$1.34460E-02$	$3.084E+11$	$1.17295E-02$	$3.084E+11$
$2.03323E-02$	$1.173E+12$	$1.60261E-02$	$1.162E+12$	$1.39806E-02$	$1.159E+12$
$2.26843E-02$	$4.408E+12$	$1.78947E-02$	$4.381E+12$	$1.56106E-02$	$4.354E+12$
$2.68735E-02$	$1.657E+13$	$2.12047E-02$	$1.651E+13$	$1.84789E-02$	$1.636E+13$
$3.57424E-02$	$6.230E+13$	$2.82703E-02$	$6.223E+13$	$2.46211E-02$	$6.146E+13$
$6.11192E-02$	$2.400E+14$	$4.84971E-02$	$2.400E+14$	$4.24178E-02$	$2.400E+14$

4. Results and discussions

The EOS models (A–H) are illustrated in Fig. 1 (which is a plot of pressure versus density). This plot refers to the high density region corresponding to the neutron star interior. We have already mentioned in section 2 the EOS that is used for the crustal region. It is important to note that because of substantial variation in the various EOS

models (A–H), the crustal thicknesses and density profiles are expected to exhibit variation even though the crustal EOS is assumed to be the same for all cases.

In Table 1, we have summarized the results for the mass (M), radius (R), central density (ρ_c), the crustal thickness (Δ) and the mass contained in the crust as a fraction of the total gravitational mass (M_{cr}/M). We have done this for three configurations of the

Table 4. Crustal density profiles: Bethe-Johnson Model V (neutrons).

$M = 1.330\ M_\odot$, $R = 10.782$ (km)		$M = 1.400\ M_\odot$, $R = 10.691$ (km)		$M = 1.658\ M_\odot$, $R = 9.200$ (km)	
$(1 - r/R)$	ρ (g cm^{-3})	$(1 - r/R)$	ρ (g cm^{-3})	$(1 - r/R)$	ρ (g cm^{-3})
$0.00000E+00$	$7.865E+00$	$0.00000E+00$	$7.865E+00$	$0.00000E+00$	$7.870E+00$
$9.62517E-10$	$1.274E+01$	$5.12115E-10$	$1.193E+01$	$1.18152E-09$	$1.483E+01$
$2.58471E-08$	$4.811E+01$	$2.15850E-08$	$4.517E+01$	$1.38593E-08$	$5.561E+01$
$1.52912E-07$	$1.817E+02$	$1.28431E-07$	$1.711E+02$	$8.06756E-08$	$2.084E+02$
$7.38784E-07$	$6.859E+02$	$6.31512E-07$	$6.479E+02$	$3.73427E-07$	$7.814E+02$
$2.60124E-06$	$2.590E+03$	$2.25472E-06$	$2.454E+03$	$1.28236E-06$	$2.929E+03$
$7.68367E-06$	$9.780E+03$	$6.70487E-06$	$9.292E+03$	$3.71389E-06$	$1.098E+04$
$2.15801E-05$	$3.693E+04$	$1.88968E-05$	$3.519E+04$	$1.03945E-05$	$4.116E+04$
$5.71082E-05$	$1.394E+05$	$5.02536E-05$	$1.333E+05$	$2.70460E-05$	$1.543E+05$
$1.40477E-04$	$5.265E+05$	$1.24064E-04$	$5.047E+05$	$6.63716E-05$	$5.784E+05$
$3.21795E-04$	$1.988E+06$	$2.85596E-04$	$1.911E+06$	$1.49243E-04$	$2.168E+06$
$6.78933E-04$	$7.507E+06$	$6.06957E-04$	$7.238E+06$	$3.10676E-04$	$8.129E+06$
$1.28251E-03$	$2.835E+07$	$1.14719E-03$	$2.741E+07$	$5.88968E-04$	$3.047E+07$
$2.30214E-03$	$1.070E+08$	$2.06531E-03$	$1.038E+08$	$1.04251E-03$	$1.142E+08$
$3.88311E-03$	$4.041E+08$	$3.49272E-03$	$3.931E+08$	$1.75488E-03$	$4.282E+08$
$6.10597E-03$	$1.526E+09$	$5.50294E-03$	$1.489E+09$	$2.75858E-03$	$1.605E+09$
$9.57620E-03$	$5.762E+09$	$8.64390E-03$	$5.638E+09$	$4.33485E-03$	$6.017E+09$
$1.44965E-02$	$2.176E+10$	$1.31203E-02$	$2.135E+10$	$6.54368E-03$	$2.256E+10$
$2.12980E-02$	$8.215E+10$	$1.92967E-02$	$8.086E+10$	$9.63627E-03$	$8.456E+10$
$2.81867E-02$	$3.102E+11$	$2.56295E-02$	$3.062E+11$	$1.27252E-02$	$3.170E+11$
$3.38868E-02$	$1.171E+12$	$3.08582E-02$	$1.160E+12$	$1.53170E-02$	$1.188E+12$
$3.78217E-02$	$4.423E+12$	$3.44667E-02$	$4.392E+12$	$1.71185E-02$	$4.454E+12$
$4.49199E-02$	$1.670E+13$	$4.09600E-02$	$1.663E+13$	$2.03358E-02$	$1.670E+13$
$5.92713E-02$	$6.306E+13$	$5.41059E-02$	$6.299E+13$	$2.71825E-02$	$6.259E+13$
$1.06539E-01$	$2.400E+14$	$9.76166E-02$	$2.400E+14$	$4.93717E-02$	$2.400E+14$

Table 5. Crustal density profiles: Walecka.

$M = 1.330\ M_\odot$ $R = 12.252$ (km)		$M = 1.400\ M_\odot$ $R = 12.280$ (km)		$M = 1.658\ M_\odot$ $R = 11.216$ (km)	
$(1 - r/R)$	ρ (g cm^{-3})	$(1 - r/R)$	ρ (g cm^{-3})	$(1 - r/R)$	ρ (g cm^{-3})
$0.00000E+00$	$7.861E+00$	$0.00000E+00$	$7.863E+00$	$0.00000E+00$	$7.873E+00$
$1.23191E-09$	$1.285E+01$	$8.38888E-10$	$1.236E+01$	$8.18035E-12$	$8.104E+00$
$3.16611E-08$	$4.842E+01$	$2.80625E-08$	$4.672E+01$	$5.39587E-09$	$3.119E+01$
$1.86840E-07$	$1.825E+02$	$1.66453E-07$	$1.766E+02$	$3.34822E-08$	$1.200E+02$
$9.00051E-07$	$6.877E+02$	$8.10853E-07$	$6.679E+02$	$1.81747E-07$	$4.621E+02$
$3.16390E-06$	$2.592E+03$	$2.87465E-06$	$2.525E+03$	$7.10899E-07$	$1.778E+03$
$9.32544E-06$	$9.767E+03$	$8.51191E-06$	$9.546E+03$	$2.18496E-06$	$6.845E+03$
$2.61696E-05$	$3.681E+04$	$2.39565E-05$	$3.609E+04$	$6.34256E-06$	$2.635E+04$
$6.91322E-05$	$1.387E+05$	$6.35046E-05$	$1.364E+05$	$1.71650E-05$	$1.014E+05$
$1.70007E-04$	$5.228E+05$	$1.56575E-04$	$5.158E+05$	$4.38472E-05$	$3.903E+05$
$3.88916E-04$	$1.970E+06$	$3.59261E-04$	$1.950E+06$	$1.03477E-04$	$1.502E+06$
$8.20653E-04$	$7.426E+06$	$7.60393E-04$	$7.373E+06$	$2.27039E-04$	$5.782E+06$
$1.54960E-03$	$2.799E+07$	$1.43749E-03$	$2.788E+07$	$4.36443E-04$	$2.225E+07$
$2.77895E-03$	$1.055E+08$	$2.58236E-03$	$1.054E+08$	$7.97867E-04$	$8.565E+07$
$4.68399E-03$	$3.975E+08$	$4.35895E-03$	$3.984E+08$	$1.36479E-03$	$3.297E+08$
$7.30487E-03$	$1.498E+09$	$6.83400E-03$	$1.506E+09$	$2.19964E-03$	$1.269E+09$
$1.15413E-02$	$5.646E+09$	$1.07640E-02$	$5.695E+09$	$3.46460E-03$	$4.884E+09$
$1.74576E-02$	$2.128E+10$	$1.62969E-02$	$2.153E+10$	$5.32332E-03$	$1.880E+10$
$2.55827E-02$	$8.019E+10$	$2.39257E-02$	$8.140E+10$	$7.89448E-03$	$7.235E+10$
$3.44452E-02$	$3.022E+11$	$3.21742E-02$	$3.078E+11$	$1.09013E-02$	$2.785E+11$
$4.11286E-02$	$1.139E+12$	$3.84200E-02$	$1.164E+12$	$1.31475E-02$	$1.072E+12$
$4.58221E-02$	$4.292E+12$	$4.28220E-02$	$4.399E+12$	$1.47359E-02$	$4.125E+12$
$5.41156E-02$	$1.618E+13$	$5.07298E-02$	$1.663E+13$	$1.74490E-02$	$1.588E+13$
$7.09277E-02$	$6.097E+13$	$6.67522E-02$	$6.287E+13$	$2.33665E-02$	$6.111E+13$
$1.17734E-01$	$2.400E+14$	$1.12973E-01$	$2.400E+14$	$4.03436E-02$	$2.400E+14$

gravitational mass, namely, 1.33 $M_\odot$, 1.4 $M_\odot$ and the maximum stable mass. A look at Table 1 shows that, for the EOS models considered here, the maximum neutron star mass (M) and their corresponding radii (R) lie in the range (1.414–2.593) $M_\odot$, and (7.082–14.096) km respectively, with the lower value of each of the quantities corresponding to the Pandharipande hyperonic matter EOS (a very soft one) and the higher

to the EOS due to Sahu, Basu & Datta (a very stiff EOS). The values of the crust thickness (Δ) for maximum mass configurations lie in the range (0.294–0.975) km. Clearly, the crust thickness, and therefore the crustal density profile, depend sensitively on the EOS model chosen to describe neutron star matter. Of the three mass configurations listed in Table 1, the $1.4\,M_\odot$ neutron star models are of particular interest because analysis of available binary pulsar data suggests the pulsar masses in

Table 6. Crustal density profiles: Friedman-Pandharipande (neutrons).

$M = 1.330\ M_\odot$, $R = 10.824$ (km)		$M = 1.400\ M_\odot$, $R = 10.701$ (km)		$M = 1.658\ M_\odot$, $R = 9.028$ (km)	
$(1 - r/R)$	ρ (g cm^{-3})	$(1 - r/R)$	ρ (g cm^{-3})	$(1 - r/R)$	ρ (g cm^{-3})
$0.00000E+00$	$7.860E+00$	$0.00000E+00$	$7.863E+00$	$0.00000E+00$	$7.861E+00$
$8.52656E-10$	$1.255E+01$	$1.37922E-09$	$1.350E+01$	$1.29813E-09$	$1.673E+01$
$2.55103E-08$	$4.744E+01$	$2.53386E-08$	$5.086E+01$	$1.12913E-08$	$6.237E+01$
$1.51130E-07$	$1.793E+02$	$1.49079E-07$	$1.915E+02$	$6.47614E-08$	$2.325E+02$
$7.33104E-07$	$6.773E+02$	$7.08975E-07$	$7.213E+02$	$2.89898E-07$	$8.667E+02$
$2.58950E-06$	$2.559E+03$	$2.46504E-06$	$2.716E+03$	$9.72901E-07$	$3.231E+03$
$7.65971E-06$	$9.671E+03$	$7.24485E-06$	$1.023E+04$	$2.78838E-06$	$1.204E+04$
$2.15325E-05$	$3.654E+04$	$2.02704E-05$	$3.852E+04$	$7.74926E-06$	$4.490E+04$
$5.70408E-05$	$1.381E+05$	$5.34425E-05$	$1.451E+05$	$1.99766E-05$	$1.674E+05$
$1.40445E-04$	$5.217E+05$	$1.30935E-04$	$5.463E+05$	$4.87008E-05$	$6.239E+05$
$3.22040E-04$	$1.971E+06$	$2.98868E-04$	$2.057E+06$	$1.09401E-04$	$2.326E+06$
$6.80500E-04$	$7.449E+06$	$6.26729E-04$	$7.748E+06$	$2.23341E-04$	$8.670E+06$
$1.28579E-03$	$2.815E+07$	$1.18248E-03$	$2.918E+07$	$4.22660E-04$	$3.232E+07$
$2.30933E-03$	$1.064E+08$	$2.11855E-03$	$1.099E+08$	$7.50797E-04$	$1.205E+08$
$3.89716E-03$	$4.019E+08$	$3.56727E-03$	$4.138E+08$	$1.24788E-03$	$4.491E+08$
$6.13009E-03$	$1.519E+09$	$5.60437E-03$	$1.558E+09$	$1.95988E-03$	$1.674E+09$
$9.61827E-03$	$5.738E+09$	$8.77043E-03$	$5.869E+09$	$3.06589E-03$	$6.241E+09$
$1.45658E-02$	$2.168E+10$	$1.32620E-02$	$2.210E+10$	$4.61747E-03$	$2.326E+10$
$2.14052E-02$	$8.193E+10$	$1.94955E-02$	$8.324E+10$	$6.80311E-03$	$8.673E+10$
$2.87813E-02$	$3.096E+11$	$2.61564E-02$	$3.135E+11$	$9.09191E-03$	$3.233E+11$
$3.43830E-02$	$1.170E+12$	$3.12389E-02$	$1.180E+12$	$1.08689E-02$	$1.205E+12$
$3.83380E-02$	$4.420E+12$	$3.48329E-02$	$4.446E+12$	$1.21344E-02$	$4.492E+12$
$4.54710E-02$	$1.670E+13$	$4.13380E-02$	$1.674E+13$	$1.43877E-02$	$1.675E+13$
$5.99013E-02$	$6.311E+13$	$5.44597E-02$	$6.305E+13$	$1.92192E-02$	$6.243E+13$
$1.04735E-01$	$2.400E+14$	$9.55692E-02$	$2.400E+14$	$3.40162E-02$	$2.400E+14$

Table 7. Crustal density profiles: Wiringa *et al.* (UV14 + UVII).

$M = 1.330\ M_\odot$ $R = 11.122$ (km)		$M = 1.400\ M_\odot$ $R = 11.115$ (km)		$M = 1.658\ M_\odot$ $R = 9.800$ (km)	
$(1 - r/R)$	ρ (g cm^{-3})	$(1 - r/R)$	ρ (g cm^{-3})	$(1 - r/R)$	ρ (g cm^{-3})
0.00000E + 00	7.865E + 00	0.00000E + 00	7.863E + 00	0.00000E + 00	7.862E + 00
4.79318E − 10	9.545E + 00	3.12246E − 11	8.123E + 00	1.33983E − 09	1.684E + 01
1.84269E − 08	3.649E + 01	1.35178E − 08	3.127E + 01	1.10568E − 08	6.274E + 01
1.14890E − 07	1.395E + 02	8.71834E − 08	1.204E + 02	6.25945E − 08	2.338E + 02
5.88007E − 07	5.332E + 02	4.62922E − 07	4.636E + 02	2.78294E − 07	8.710E + 02
2.21576E − 06	2.038E + 03	1.81126E − 06	1.785E + 03	9.35252E − 07	3.246E + 03
6.74056E − 06	7.792E + 03	5.62199E − 06	6.872E + 03	2.67672E − 06	1.209E + 04
1.92271E − 05	2.979E + 04	1.61628E − 05	2.646E + 04	7.43546E − 06	4.506E + 04
5.19015E − 05	1.139E + 05	4.41569E − 05	1.019E + 05	1.91534E − 05	1.679E + 05
1.29966E − 04	4.353E + 05	1.11643E − 04	3.922E + 05	4.66804E − 05	6.256E + 05
3.03771E − 04	1.664E + 06	2.64122E − 04	1.510E + 06	1.04872E − 04	2.331E + 06
6.60309E − 04	6.361E + 06	5.82289E − 04	5.813E + 06	2.13857E − 04	8.686E + 06
1.25384E − 03	2.432E + 07	1.11103E − 03	2.238E + 07	4.04672E − 04	3.236E + 07
2.27729E − 03	9.295E + 07	2.03311E − 03	8.617E + 07	7.18723E − 04	1.206E + 08
3.88460E − 03	3.553E + 08	3.49593E − 03	3.318E + 08	1.20173E − 03	4.493E + 08
6.17831E − 03	1.358E + 09	5.61392E − 03	1.277E + 09	1.87529E − 03	1.674E + 09
9.70251E − 03	5.193E + 09	8.77612E − 03	4.918E + 09	2.93350E − 03	6.238E + 09
1.48127E − 02	1.985E + 10	1.34625E − 02	1.893E + 10	4.41814E − 03	2.324E + 10
2.18186E − 02	7.588E + 10	1.99008E − 02	7.290E + 10	6.50913E − 03	8.661E + 10
2.97300E − 02	2.901E + 11	2.73359E − 02	2.807E + 11	8.70128E − 03	3.227E + 11
3.56409E − 02	1.109E + 12	3.28536E − 02	1.081E + 12	1.04031E − 02	1.203E + 12
3.97973E − 02	4.239E + 12	3.67344E − 02	4.160E + 12	1.16147E − 02	4.481E + 12
4.71200E − 02	1.620E + 13	4.35051E − 02	1.602E + 13	1.37662E − 02	1.670E + 13
6.18097E − 02	6.195E + 13	5.71556E − 02	6.167E + 13	1.83039E − 02	6.221E + 13
1.00741E − 01	2.400E + 14	9.34953E − 02	2.400E + 14	2.99743E − 02	2.400E + 14

these binaries to be close to this value. For the 1.4 $M_\odot$ models, the Δ is in the range (0.361–2.970) km, a much wider range than for the maximum mass cases. In Tables 2–9, we give the crustal density variation with the depth in normalized units with respect to the radius $(1 - r/R)$, (where r is the radial distance from the centre of the star) from the surface of the neutron star for the three mass configurations. These tables will be of direct application in calculations of magnetic field evolution of pulsars. The same thing,

namely, the crustal density variations, is graphically illustrated in Figs. 2 and 3 for $1.4\,M_\odot$ configurations for the various EOS models. The dashed lines in these figures represent the core-inner crust boundary (which corresponds to $r = R - \Delta$) and the dot-cum-dashed lines represent the surface of the neutron star ($r = R$). The variation is sharpest for the softest EOS considered here (Pandharipande hyperonic matter) and gets to be comparatively less sharp as the EOS gets to be more stiff. The dependences on

Table 8. Crustal density profiles: Prakash, Ainsworth & Lattimer Model 1.

$M = 1.330\ M_\odot$ $R = 11.384$ (km)		$M = 1.400\ M_\odot$ $R = 10.987$ (km)		$M = 1.658\ M_\odot$ $R = 9.483$ (km)	
$(1 - r/R)$	ρ (g cm^{-3})	$(1 - r/R)$	ρ (g cm^{-3})	$(1 - r/R)$	ρ (g cm^{-3})
$0.00000E+00$	$7.864E+00$	$0.00000E+00$	$7.861E+00$	$0.00000E+00$	$7.868E+00$
$1.23204E-09$	$1.299E+01$	$5.64384E-10$	$1.202E+01$	$7.20466E-10$	$1.297E+01$
$2.87558E-08$	$4.893E+01$	$2.26968E-08$	$4.539E+01$	$1.70600E-08$	$4.893E+01$
$1.69510E-07$	$1.843E+02$	$1.34550E-07$	$1.714E+02$	$1.00739E-07$	$1.846E+02$
$8.13995E-07$	$6.945E+02$	$6.59261E-07$	$6.476E+02$	$4.84015E-07$	$6.966E+02$
$2.85212E-06$	$2.616E+03$	$2.34711E-06$	$2.446E+03$	$1.70821E-06$	$2.628E+03$
$8.40799E-06$	$9.857E+03$	$6.97231E-06$	$9.238E+03$	$5.00958E-06$	$9.917E+03$
$2.35563E-05$	$3.713E+04$	$1.95999E-05$	$3.489E+04$	$1.41327E-05$	$3.742E+04$
$6.22494E-05$	$1.399E+05$	$5.20863E-05$	$1.318E+05$	$3.71474E-05$	$1.412E+05$
$1.52771E-04$	$5.270E+05$	$1.28304E-04$	$4.978E+05$	$9.18752E-05$	$5.327E+05$
$3.49639E-04$	$1.986E+06$	$2.95396E-04$	$1.880E+06$	$2.08710E-04$	$2.010E+06$
$7.37203E-04$	$7.480E+06$	$6.28698E-04$	$7.102E+06$	$4.40124E-04$	$7.585E+06$
$1.39012E-03$	$2.818E+07$	$1.18548E-03$	$2.683E+07$	$8.35840E-04$	$2.862E+07$
$2.49418E-03$	$1.062E+08$	$2.13488E-03$	$1.013E+08$	$1.48947E-03$	$1.080E+08$
$4.20487E-03$	$4.000E+08$	$3.61133E-03$	$3.827E+08$	$2.51514E-03$	$4.074E+08$
$6.60710E-03$	$1.507E+09$	$5.69228E-03$	$1.446E+09$	$3.95905E-03$	$1.537E+09$
$1.04093E-02$	$5.677E+09$	$8.98241E-03$	$5.460E+09$	$6.24693E-03$	$5.801E+09$
$1.56800E-02$	$2.139E+10$	$1.35685E-02$	$2.062E+10$	$9.43094E-03$	$2.189E+10$
$2.29656E-02$	$8.057E+10$	$1.99082E-02$	$7.790E+10$	$1.38631E-02$	$8.258E+10$
$3.27849E-02$	$3.036E+11$	$2.85376E-02$	$2.942E+11$	$1.98362E-02$	$3.116E+11$
$3.71907E-02$	$1.144E+12$	$3.26160E-02$	$1.111E+12$	$2.24955E-02$	$1.176E+12$
$4.15513E-02$	$4.308E+12$	$3.63684E-02$	$4.198E+12$	$2.51423E-02$	$4.436E+12$
$4.96169E-02$	$1.623E+13$	$4.34154E-02$	$1.586E+13$	$3.01974E-02$	$1.674E+13$
$6.63662E-02$	$6.115E+13$	$5.79696E-02$	$5.989E+13$	$4.11830E-02$	$6.316E+13$
$1.49536E-01$	$2.400E+14$	$1.32527E-01$	$2.400E+14$	$9.50182E-02$	$2.400E+14$

Table 9. Crustal density profiles: Sahu, Basu & Datta.

$M = 1.330\ M_\odot$ $R = 14.685$ (km)		$M = 1.400\ M_\odot$ $R = 14.761$ (km)		$M = 1.658\ M_\odot$ $R = 14.096$ (km)	
$(1 - r/R)$	ρ (g cm^{-3})	$(1 - r/R)$	ρ (g cm^{-3})	$(1 - r/R)$	ρ (g cm^{-3})
$0.00000E+00$	$7.861E+00$	$0.00000E+00$	$7.861E+00$	$0.00000E+00$	$7.863E+00$
$1.68177E-10$	$8.839E+00$	$6.18207E-10$	$1.139E+01$	$1.28531E-09$	$1.483E+01$
$2.51686E-08$	$3.391E+01$	$3.29844E-08$	$4.323E+01$	$1.50712E-08$	$5.553E+01$
$1.54202E-07$	$1.301E+02$	$1.96946E-07$	$1.640E+02$	$8.76310E-08$	$2.080E+02$
$8.19531E-07$	$4.990E+02$	$9.80469E-07$	$6.220E+02$	$4.05511E-07$	$7.789E+02$
$3.13725E-06$	$1.914E+03$	$3.54032E-06$	$2.360E+03$	$1.39181E-06$	$2.917E+03$
$9.61781E-06$	$7.344E+03$	$1.05575E-05$	$8.951E+03$	$4.02961E-06$	$1.092E+04$
$2.75907E-05$	$2.817E+04$	$2.98693E-05$	$3.396E+04$	$1.12695E-05$	$4.091E+04$
$7.48055E-05$	$1.081E+05$	$7.95623E-05$	$1.288E+05$	$2.93190E-05$	$1.532E+05$
$1.88519E-04$	$4.146E+05$	$1.97315E-04$	$4.886E+05$	$7.19116E-05$	$5.737E+05$
$4.42469E-04$	$1.591E+06$	$4.54910E-04$	$1.854E+06$	$1.61745E-04$	$2.149E+06$
$9.61559E-04$	$6.102E+06$	$9.64816E-04$	$7.032E+06$	$3.36900E-04$	$8.046E+06$
$1.84383E-03$	$2.341E+07$	$1.83881E-03$	$2.667E+07$	$6.38253E-04$	$3.013E+07$
$3.35559E-03$	$8.979E+07$	$3.31124E-03$	$1.012E+08$	$1.13022E-03$	$1.128E+08$
$5.73697E-03$	$3.445E+08$	$5.60155E-03$	$3.839E+08$	$1.90195E-03$	$4.226E+08$
$9.15009E-03$	$1.321E+09$	$8.77845E-03$	$1.456E+09$	$2.98755E-03$	$1.583E+09$
$1.43445E-02$	$5.069E+09$	$1.38724E-02$	$5.524E+09$	$4.69758E-03$	$5.927E+09$
$2.18743E-02$	$1.945E+10$	$2.10140E-02$	$2.095E+10$	$7.09328E-03$	$2.220E+10$
$3.21388E-02$	$7.460E+10$	$3.07877E-02$	$7.949E+10$	$1.04322E-02$	$8.313E+10$
$4.41761E-02$	$2.862E+11$	$4.18584E-02$	$3.015E+11$	$1.41597E-02$	$3.113E+11$
$5.25674E-02$	$1.098E+12$	$4.96901E-02$	$1.144E+12$	$1.68582E-02$	$1.166E+12$
$5.85730E-02$	$4.212E+12$	$5.53066E-02$	$4.339E+12$	$1.88106E-02$	$4.366E+12$
$6.90648E-02$	$1.616E+13$	$6.52886E-02$	$1.646E+13$	$2.22586E-02$	$1.635E+13$
$9.05533E-02$	$6.198E+13$	$8.55960E-02$	$6.245E+13$	$2.95893E-02$	$6.123E+13$
$2.13000E-01$	$2.400E+14$	$2.01202E-01$	$2.400E+14$	$6.91727E-02$	$2.400E+14$

neutron star mass of the radius and of the crustal thickness respectively are illustrated in Figs. 4 and 5. From Fig. 4, it can be seen that for the EOS models Walecka (1974), and Sahu, Basu & Datta (1993), i.e. curves D and H, the slope for the lower values of the stable mass is noticeably positive. This is because of the substantial contribution of attractive force brought on by the scalar σ-meson interaction present in these equations of state. It may be mentioned here that the σ-interaction plays an important role at

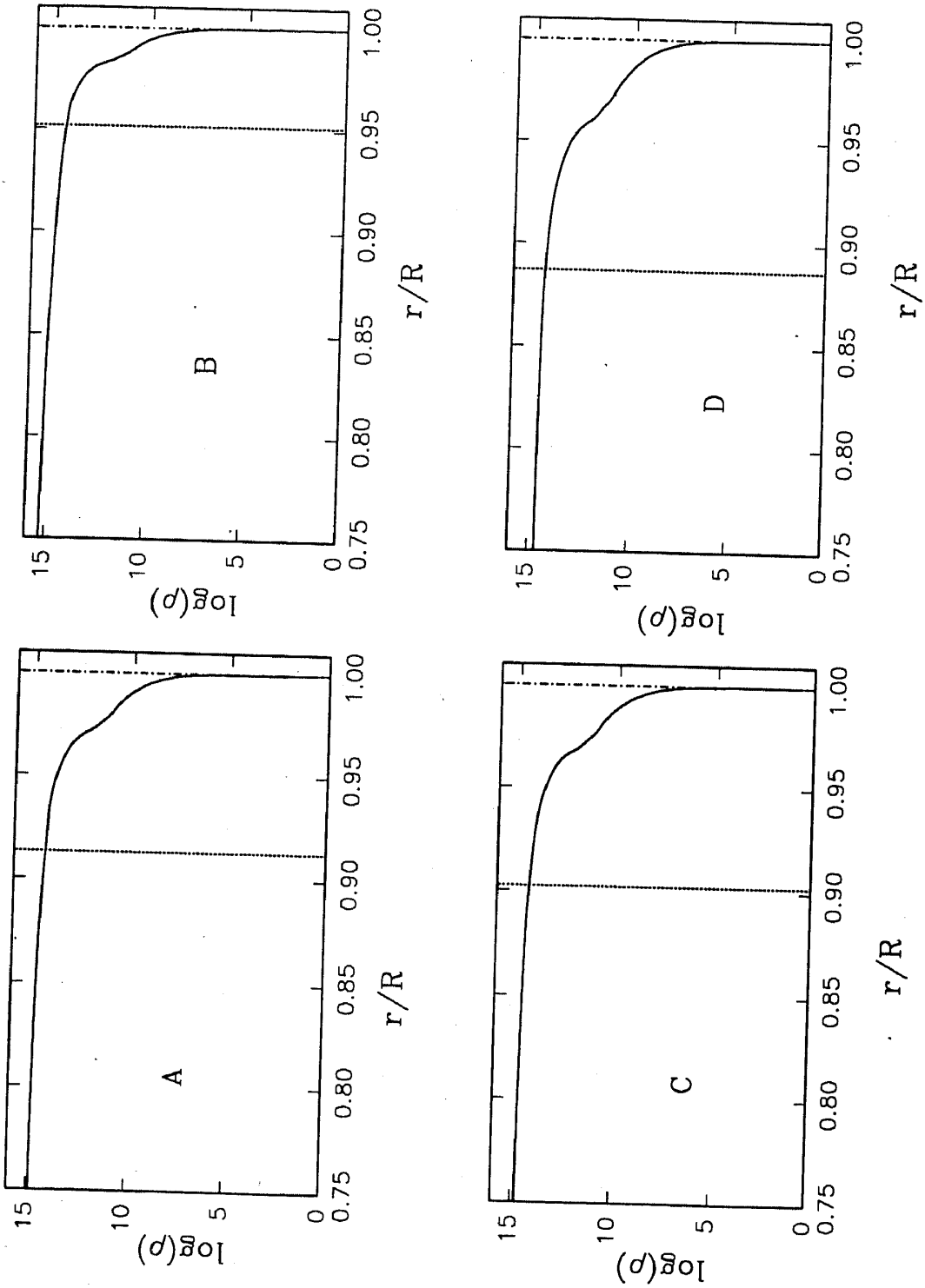

Figure 2. Neutron star density profiles for 1.4 $M_{\odot}$: EOS models (A–D).

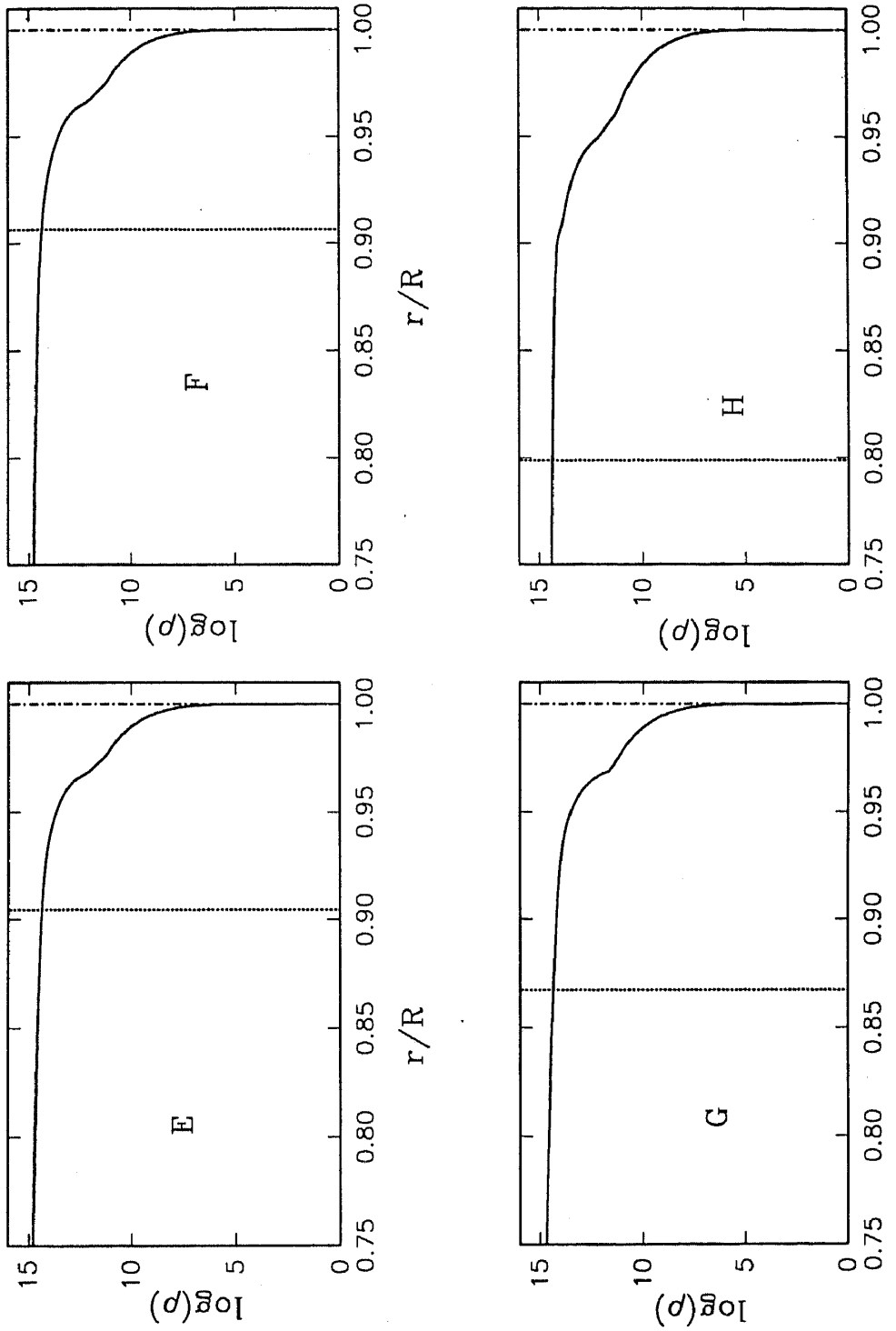

Figure 3. Neutron star density profiles for 1.4 $M_{\odot}$: EOS models (E–H).

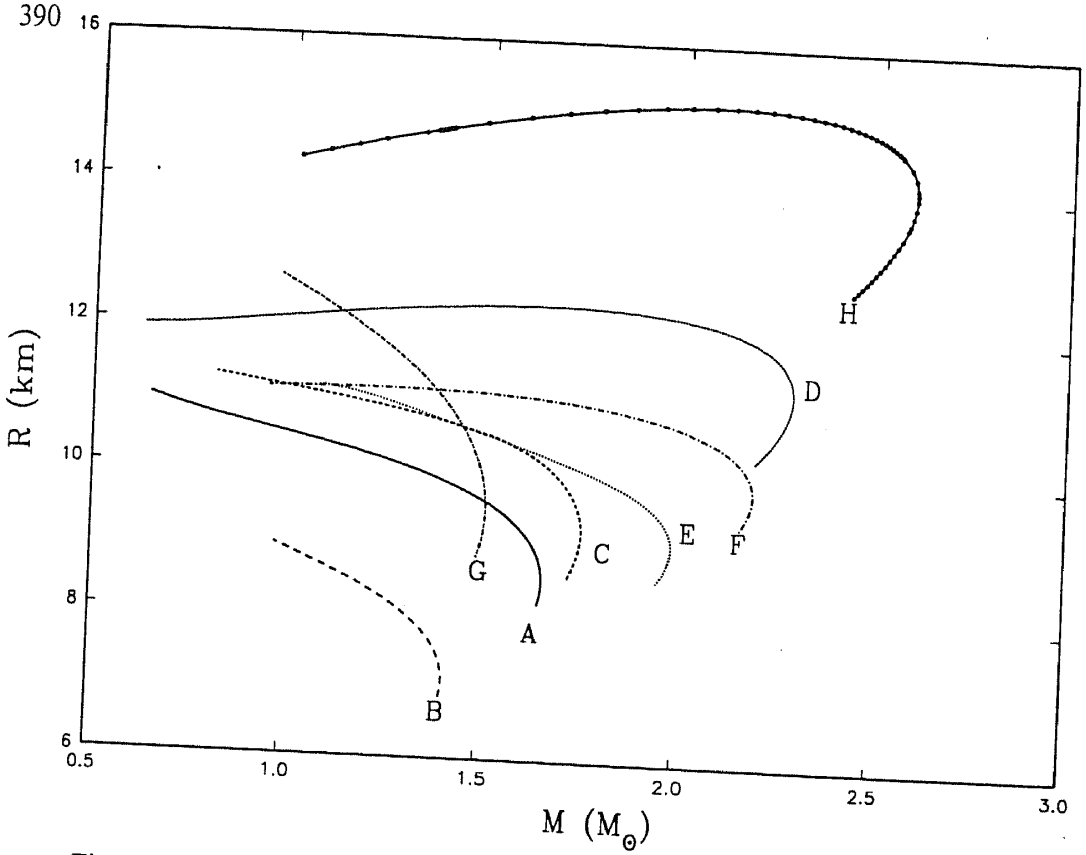

Figure 4. Neutron star mass-radius dependences for the EOS models (A–H).

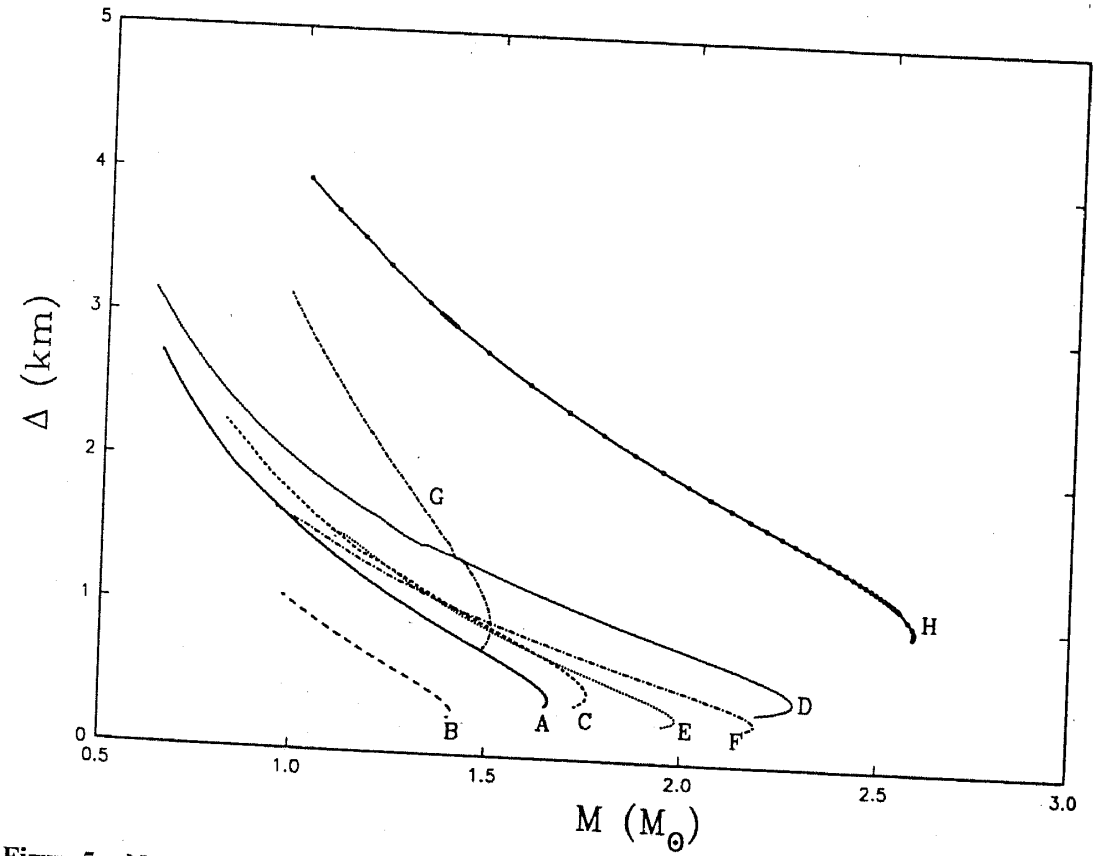

Figure 5. Neutron star crustal thickness (Δ) as a function of the gravitational mass (M) for the EOS models (A–H).

intermediate densities providing nuclear saturation, and must be included in any field theoretical EOS model. At high densities the contribution of the vector meson (ω) interaction, which provides repulsive force dominates, and the slope becomes negative. The crustal thickness (Δ) is decided by how much mass is contained in the core and interior regions of the neutron star, so that, in general, the more the mass of the neutron star, the less the value of Δ for any EOS.

As already emphasized, the crustal density profile of neutron stars is a key input in the proper understanding of a variety of important features associated with pulsars, such as the cooling rate. Another important application, that is of much current interest in astrophysics, relates to the evolution of magnetic fields of pulsars. However, several calculations reported in the literature on the problem of magnetic field evolution have considered cooling models for a specific EOS model while using the crustal model that corresponds to a different EOS model. This is mainly because of non-availability of detailed, numerical crustal density profiles. The survey presented here is a preliminary step towards a uniform and consistent investigation of the problem of evolution of neutron star magnetic fields, which will be reported in a forthcoming paper (Bhattacharya & Datta 1995).

Acknowledgement

B. Datta thanks the Director, Raman Research Institute for the kind hospitality.

References

Ambartsumyan, V. A., Saakyan, G. S. 1960, *Soviet Astr.*, **4**, 187.
Antia, H. M. 1991, *Numerical Methods for Scientists & Engineers* (New Delhi: Tata McGraw Hill Publ.) 895.
Arnett, W. D., Bowers, R. L. 1977, *Astrophys. J. Suppl.*, **33**, 415.
Baym, G., Pethick, C. J., Sutherland, P. G. 1971, *Astrophys. J.*, **170**, 299.
Bethe, H. A., Johnson, M. B. 1974, *Nucl. Phys.*, **A230**, 1.
Bhattacharya, D., Datta, B. 1995, preprint.
Datta, B. 1988, *Fund. Cosmic Phys.*, **12**, 151.
Feynman, R. P., Metropolis, N., Teller, E. 1949, *Phys. Rev.*, **75**, 1561.
Friedman, B., Pandharipande, V. R. 1981, *Nucl. Phys.*, **A361**, 502.
Jastrow, R. 1955, *Phys. Rev.*, **98**, 1479.
Möller, P., Myers, W. D., Swiatecki, M. J., Treiner, J. 1988, *Atomic Data Nucl. Data Tables* **39**, 225.
Negele, J. W., Vautherin, D. 1973, *Nucl. Phys.*, **A207**, 298.
Oppenheimer, J. R., Volkoff, G. M. 1939, *Phys. Rev.*, **55**, 374.
Pandharipande, V. R. 1971a, *Nucl. Phys.*, **A174**, 641.
Pandharipande, V. R. 1971b, *Nucl. Phys.*, **A178**, 123.
Prakash, M., Ainsworth, T. L., Lattimer, J. M. 1988, *Phys. Rev. Lett.*, **61**, 2518.
Reid, R. V., Jr. 1968, *Ann. Phys.*, **50**, 411.
Sahu, P. K., Basu, R., Datta, B. 1993, *Astrophys. J.*, **416**, 267.
Walecka, J. D. 1974, *Ann. Phys.*, **83**, 491.
Wiringa, R. B., Fiks, V., Fabrocini, A, 1988, *Phys. Rev. C*, **38**, 1010.